

# Responses of Phytoplankton Communities to Environmental Variability in the East China Sea

Xin Liu,<sup>1,2,3</sup> Wupeng Xiao,<sup>1</sup> Michael R. Landry,<sup>2</sup> Kuo-Ping Chiang,<sup>3</sup>  
Lei Wang,<sup>1</sup> and Bangqin Huang<sup>1\*</sup>

<sup>1</sup>State Key Laboratory of Marine Environmental Science/Key Laboratory of Coastal and Wetland Ecosystems, Ministry of Education, Xiamen University, Xiamen 361005, Fujian, China; <sup>2</sup>Scripps Institution of Oceanography, University of California at San Diego, La Jolla, CA 92195, USA; <sup>3</sup>Institute of Marine Environmental Chemistry and Ecology, National Taiwan Ocean University, 202-24 Keelung, Taiwan, China

## ABSTRACT

We investigated seasonal and spatial patterns of phytoplankton variability in the East China Sea in order to understand biomass and compositional responses to environmental factors in the contemporary ocean. We used satellite imagery from 2002 to 2013 to define the mean seasonal climatology of sea surface temperature and chlorophyll *a*. Phytoplankton and environmental measurements were synthesized for the study region and four seasons from 11 cruises conducted from 2006 to 2012. The results of CHEMTAX analyses on group-specific phytoplankton composition were consistent with those of microscopy and flow cytometry observations, revealing three patterns of seasonal variability. Canonical correspondence analysis and generalized additive models (GAMs) were used to resolve the spatiotemporal variations of major phytoplankton groups and their relationships to

month, temperature, salinity, nutrients, mixed layer depth, and bottom depth. Monsoon forcing drove the distributional patterns of environmental factors and was critical to explaining phytoplankton dynamics at the seasonal scale. Compared to autumn and winter, significantly higher chlorophyll *a* concentrations were observed during spring and summer, associated with the spring bloom and the Changjiang (Yangtze) River plume, respectively. Diatoms dominated biomass over the East China Sea, especially during the summer months influenced by the Changjiang (Yangtze) River plume, whereas dinoflagellates were especially important during spring blooms. GAMs analysis showed the differences in their responses to environmental variability, with a clear mid-range salinity optimum (~31) and a more pronounced temperature effect for dinoflagellates. The photosynthetic bacteria, *Prochlorococcus* and *Synechococcus*, both increased strongly with warming, but *Prochlorococcus* showed stronger sensitivity to variations in physical environmental parameters, whereas *Synechococcus* was more responsive to chemical (nutrient) variability, with broader tolerance of low-salinity conditions.

Received 22 June 2015; accepted 15 January 2016;  
published online 18 April 2016

Xin Liu and Wupeng Xiao have contributed equally to this work.

**Author contributions** X. Liu and W. Xiao contributed equally to this paper for their leading roles in field sampling and writing of the manuscript. B. Huang initially designed the study and supervised the projects. M. Landry and K.P. Chiang contributed to the data analysis. L. Wang contributed to field sampling as well. This study was conceived in discussion between all authors.

\*Corresponding author; e-mail: bqhuang@xmu.edu.cn

**Key words:** phytoplankton; community structure; East China Sea; environmental factors; canonical correspondence analysis; generalized additive models.

## INTRODUCTION

Phytoplankton contribute about half of all photosynthetic activity on Earth (Field and others 1998), sustaining the aquatic food web and its biogeochemical cycles. With growing evidence of climate change and other anthropogenic impacts, future scenarios for phytoplankton in ocean ecosystems are matters of great interest and concern (Boyce and others 2010; Anderson and others 2012; Doney and others 2012). In coastal systems, increased wind-driven upwelling (Bakun 1990) and anthropogenic nutrient inputs (Jiang and others 2014; Kim and others 2014) may increase blooms of larger phytoplankton (Falkowski and Oliver 2007; Glibert and others 2014) and possibly harmful species (Zhou and others 2008; Jiang and others 2014). In contrast, increasing thermal stratification in open-ocean systems will likely result in decreased nutrient availability and biomass (Boyce and others 2010) and selection for smaller cells (Moran and others 2010; Flombaum and others 2013). In addition, phytoplankton communities are diverse polyphyletic assemblages of lineages that differ in origin, evolutionary age, and modern distributions (Falkowski and others 2004). Even among phytoplankton species of similar size, entirely different food-web structures and production can be observed, depending on composition of dominant species and groups and their varying life history strategies (Litchman and others 2007). Much effort has gone into defining potential ecosystem responses to global change from projected changes in phytoplankton composition (Falkowski and Oliver 2007; Behrenfeld 2011; Chavez and others 2011). The final outcomes, however, remain uncertain. Understanding the integrated consequences of future changes will require a comprehensive and multi-stressor evaluation of plankton ecosystem responses and feedbacks (Behrenfeld and others 2015; Boyd and others 2015).

The East China Sea is a unique marginal sea that includes a large area of shallow continental shelf that receives strong influences from nutrient-rich fresh water of the Changjiang (Yangtze) River, as well as from subtropical open-ocean waters of the Kuroshio Current (Gong and others 1996). Seasonal dynamics of the East China Sea are driven by wind-forcing associated with the East Asian Monsoon (Gong and others 2003), with upwelling and plume favorable southwest winds during summer and strong deep-mixing winds from the northeast during winter. Phytoplankton biomass, production,

and community structure are thus highly variable seasonally and spatially in the East China Sea (Gong and others 1996; Furuya and others 2003; Gong and others 2003; Yamaguchi and others 2012), providing an ideal setting to study the associations and responses of different phytoplankton groups to environmental factors.

Recent studies have described the general distributions of large (Chiang and others 1999, 2004; Guo and others 2014b) and small phytoplankton (Jiao and others 1998; Chiang and others 2002; Jiao and others 2002, 2005; Guo and others 2014a) in the East China Sea. As elsewhere, there are higher biomass and larger seasonal variations inshore and lower biomass and reduced temporal variability offshore. Large phytoplankton dominate inshore and during winter, and small phytoplankton dominate offshore and during summer. Although these general patterns suggest that there are specific relationships that define how various components of phytoplankton communities align with environmental conditions and respond to change in the East China Sea, this kind of synthetic analysis has not previously been attempted.

Here, we combine analyses of long-term satellite data with field measurements from 11 cruises covering the continental shelf area and four seasons in the East China Sea. Using canonical correspondence analysis (CCA) and generalized additive models (GAMs), we resolve the spatiotemporal variations of major phytoplankton groups and their relationships to environmental factors. These results are then used to address the following questions: (i) what are the seasonal patterns of phytoplankton community structure in different water masses in the East China Sea, (ii) how do environmental factors influence phytoplankton distributions, and (iii) what are the implications for future trends?

## MATERIALS AND METHODS

We synthesize data from eleven cruises conducted in the East China Sea from November 2006 to August 2012 during the three projects supported by the National Basic Research Programs of China (973 Program) (Table 1). Figure 1A shows all of the sampling stations for these cruises, which cover the entire continental shelf area and four seasons. Sampling stations were located irregularly in space and varied among cruises, with data density greatest in the dynamic region near the Changjiang (Yangtze) River estuary and adjacent waters (Figure 1A). Each season is represented by at least

2 years of sampling, greater than 400 sampling stations and >1500 samples analyzed (Table 1).

At each station, a vertical profile of photosynthetically active radiation (PAR) was made using a free-fall spectroradiometer (SPMR, Satlantic) just prior to water sampling. Hydrographic measurements and water samples were then collected using a Seabird CTD profiler equipped with a 12 Niskin bottle rosette sampler. All samples were taken in the euphotic zone from at least three layers: the surface water ( $\leq 5$  m), the subsurface chlorophyll *a* maximum, and the bottom of the euphotic zone. The euphotic zone was defined as the water column down to the depth at which the downward PAR was 1% of the value just below the surface. Mixed layer depth (MLD) was determined as the first depth where seawater density exceeded the density at 5 m by  $0.125 \text{ kg m}^{-3}$  (Thomson and Fine 2003).

Nutrient samples from cruises C1–C4 were analyzed on shipboard using a four-channel continuous-flow Technicon AA3 AutoAnalyzer (Bran-Lube GmbH) (Han and others 2012). Nutrient samples for cruises E1–E3 were filtered immediately after collection through acid-cleaned  $0.45\text{-}\mu\text{m}$  pore size acetate cellulose filters; the filtrates were poisoned with saturated  $\text{HgCl}_2$  solution and frozen at  $-20^\circ\text{C}$ . Nutrient concentrations were later determined using a Skalar SAN<sup>plus</sup> Autoanalyzer (Liu and others 2009). The precision for nutrient analyses in this study was  $\leq 3\%$ , and the detection limits for  $\text{NO}_3^- + \text{NO}_2^- (\text{NO}_x^-)$ , soluble reactive phosphate (SRP), and  $\text{Si}(\text{OH})_4$  (silicic acid) analyses were 0.03, 0.03, and  $0.05 \mu\text{mol l}^{-1}$ , respectively, for shipboard analyses (C1–C4) and 0.06, 0.03, and  $0.15 \mu\text{mol l}^{-1}$ , respectively, for the land-based analyses (E1–E3) (Liu and others 2009; Han and

others 2012). Nutrient results are not available for the J1–J4 cruises in 2011–2012.

Photosynthetic pigment concentrations were measured by high-performance liquid chromatography (HPLC) (Zapata and others 2000; Furuya and others 2003). These results were then used to calculate the relative contributions of different phytoplankton groups to total chlorophyll *a* (TChl *a*) based on the CHEMTAX approach (Mackey and others 1996). We used CHEMTAX calculations and procedures as described by Latasa (2007), with the input pigment ratio matrix based on pigment relationships for common phytoplankton groups from previous studies in the East China Sea and adjacent waters (Liu and others 2012, 2015b).

Mean seasonal estimates of sea surface temperature (SST) and TChl *a* were extracted from daily MODIS/Aqua data covering the study region from July 2002 to December 2013 (Figures 2, 3). The raw TChl *a* data were processed by the NASA Goddard Space Flight Center (GSFC) using similar atmospheric correction algorithms as for SeaWiFS (Collection 4) but with the OC3 bio-optical algorithm (Zhang and others 2006). A one-way ANOVA was used for statistical analysis to compare the difference among seasons using the Duncan method, which accommodates unequal group sizes. The significance level was set at  $P < 0.05$ . To relate phytoplankton community composition to environmental variables, we performed a CCA, which is an eigenvector technique for multivariate direct gradient analysis (Ter Braak 1986). The R package 'Vegan' was used to perform the regularized extension of CCA (Oksanen 2015). The CCA results are presented as variable plots that describe the seasonal patterns of correlations between group-specific phytoplankton chlorophyll *a* con-

**Table 1.** Summary of Sample Collections during 11 Cruises in the East China Sea

Cruise	Dates	Season	Stations	Samples
E1	26 Nov–13 Dec 2006	Late autumn	29	104
E2	24 Feb–10 Mar 2007	Late winter	28	128
E3	12–20 May 2008	Spring	25	97
C1	19–27 Aug 2009	Summer	55	350
C2	23 Dec 2009–4 Jan 2010	Winter	59	285
C3	27 Nov–9 Dec 2010	Late autumn	52	204
J1	8–20 Apr 2011	Spring	42	205
C4	29 May–8 Jun 2011	Late spring	58	231
J2	11–27 Aug 2011	Summer	41	170
J3	9–24 Jun 2012	Summer	28	171
J4	11–24 Aug 2012	Summer	13	61

The letters E, C, and J refer to cruises funded by the China GLOBEC-IMBER Program, the China Ocean Carbon Program (CHOICE-C), and the China Jellyfish Program, respectively. Listed are cruise dates, season, number of stations sampled, and number of phytoplankton samples analyzed.

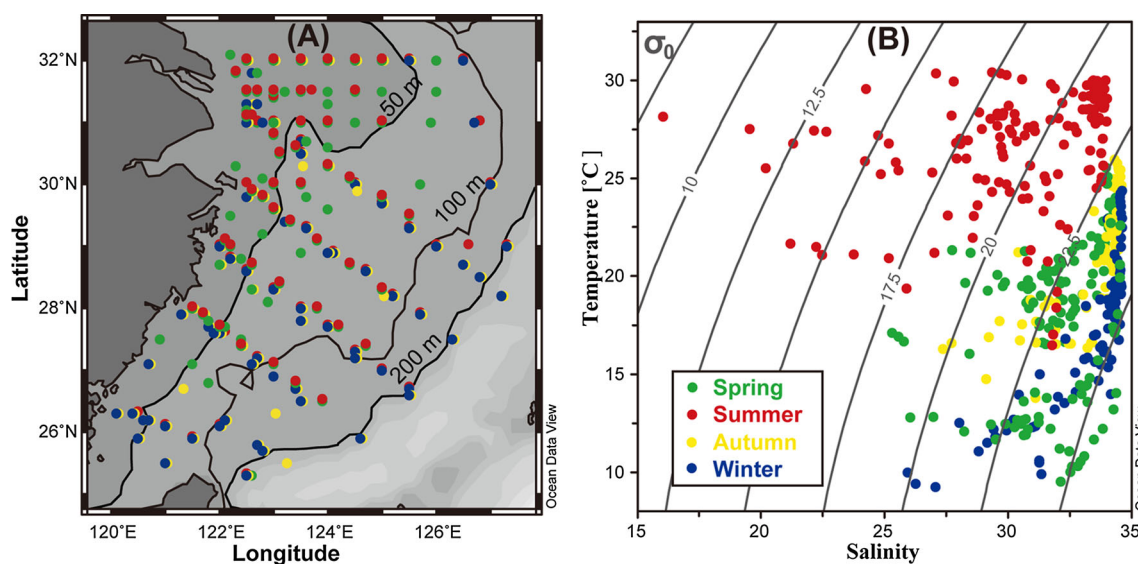


**Figure 1.** Map of sampling stations (A) and temperature-salinity (T-S) diagram of surface water samples (B) from 11 cruises in the East China Sea from 2006 to 2012. The isobaths of 50, 100, and 200 m are indicated by the *black solid lines*. *Color code* denotes season of sampling. Specific cruise dates and sample numbers are given in Table 1.

centrations (natural logarithmic transformation) and environmental factors. We also used GAMs to obtain further insights into the relationships between response and explanatory variables (Wood 2006; Zuur and others 2007). We constructed GAMs with a Gamma distributions to fit the data on effects of temperature, salinity, nutrient concentration ( $\text{NO}_x$ ), and month using the function ‘gam’ in the R package ‘mgcv,’ which assumes that the effects of each predictor on the response variable can be described by smooth functions (Hastie and Tibshirani 1986; Wood 2006; R 2015). As some of these predictors may correlate closely with each other (for example, temperature and nutrients), leading to equivocal interpretations (Irwin and others 2012), we used just one parameter at a time and established GAM formations as follows:

$$Y = \alpha + s(X) + \varepsilon$$

where  $Y$  represents the chlorophyll  $a$  concentrations of four dominant phytoplankton groups (diatoms, dinoflagellates, *Synechococcus*, and *Prochlorococcus*) based on their diagnostic pigments fucoxanthin, peridinin, zeaxanthin, and divinylchlorophyll  $a$ , respectively,  $X$  represents the four explanatory parameters (month, temperature, salinity, and  $\text{NO}_x$ ), and  $\alpha$  is the grand mean or intercept. One-dimensional nonlinear functions based on cubic regression spline were used for each smoother functions (Wood 2006). To avoid overfitting, the maximum number of basis functions was constrained at five, except for peridinin against

$\text{NO}_x$ . Peridinin was not significantly correlated with  $\text{NO}_x$  until the number of basis functions was increased to nine. These calculations can be seen in detail in previous studies (Chen and others 2012, 2014). Based upon relative importance and sufficient information, the present study focused on comparisons between diatom and dinoflagellates, and between *Synechococcus* and *Prochlorococcus*. In addition, because of the variability of phytoplankton photosynthetic pigments with light level in the water column, we mainly based the present results on samples collected in the surface layer (0–5 m,  $n = 426$ ).

## RESULTS

### Seasonal Variability of SST and Tchl $a$

Satellite imagery from July 2002 to December 2013 was used to define the mean seasonal climatology of sea surface temperature (SST, Figure 2) and Tchl  $a$  (Figure 3) in the East China Sea during our study period. Two distributional patterns of SST can be observed. During spring and winter, SST increases from north to south and from the near-shore to offshore (Figure 2). During summer and fall, SST is high and relatively uniform in the range of 26–30°C, except for a slightly cooler region near around the Zhoushan Islands that separate Hangzhou Bay from the East China Sea (Figure 2B). In contrast to SST, spatial gradients in Tchl  $a$  concentration are large, exceeding an order of magni-



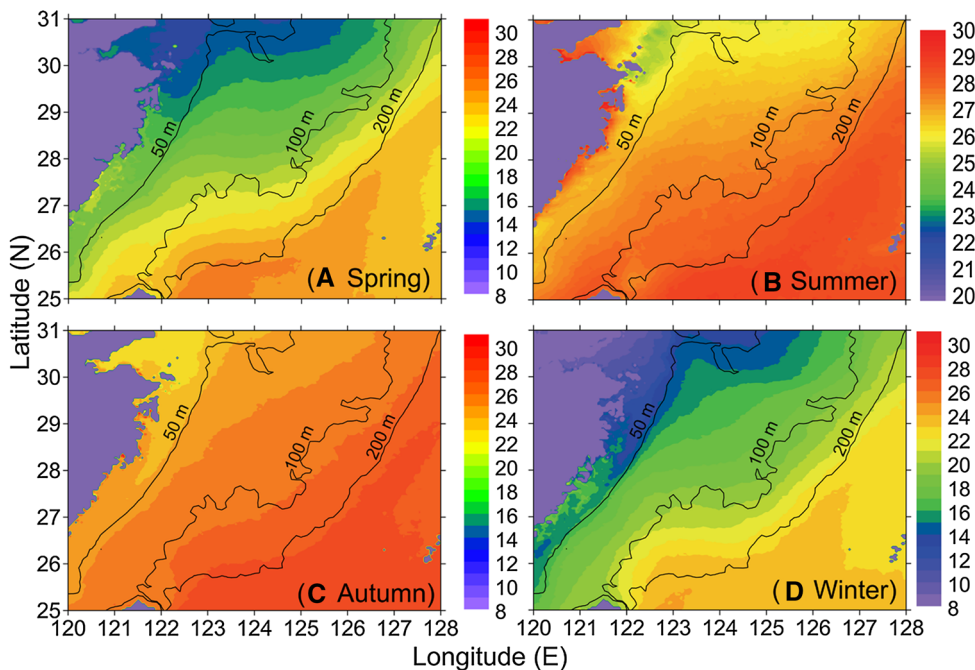


Figure 2. Climatological mean seasonal values of sea surface temperature (SST, °C) in the East China Sea from July 2002 to December 2013.

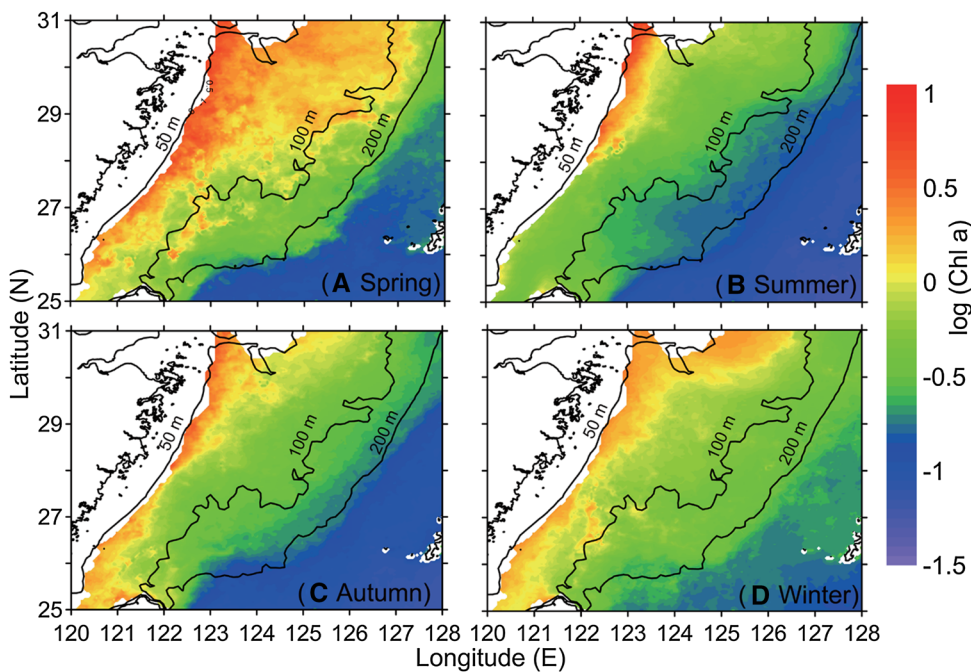


Figure 3. Climatological mean seasonal values of sea surface chlorophyll *a* ( $\mu\text{g l}^{-1}$ ) in the East China Sea from July 2002 to December 2013. Seasonal averages are derived from MODIS/Aqua imagery with the OC3 bio-optical algorithm.

tude, during all seasons (Figure 3). Mean Tchl *a* concentrations of  $2\text{--}3 \mu\text{g l}^{-1}$  occur in the near-coastal area throughout the year and more extensively over the continental shelf during springtime (Figure 3A). In the offshore region bordering the Kuroshio Current (depth > 200 m), the seasonal pattern is opposite, with the lowest mean Tchl *a* of about  $0.1 \mu\text{g l}^{-1}$  in summer and the highest average in winter ( $\sim 0.5 \mu\text{g l}^{-1}$ ).

### Temperature-Salinity, Nutrient, and Chlorophyll Relationships

As observed in T-S diagram of surface waters in Figure 1B, hydrographic properties are most similar between late autumn and winter cruises and more variable in spring and summer cruises, during which there is a strong seasonal shift to the higher temperatures and lower salinities observed during

summer. Seasonal differences are mainly reflected in the variations of temperature, whereas spatial variability is most prominent in salinity, especially in relation to the coastal area of river influence. According to the T-S diagram analysis and previous studies (Gong and others 1996; Chen 2009), three water masses can be classified for the East China Sea region (Table 2): the Changjiang River plume (salinity < 31), the East China Sea mid-shelf surface water (salinity 31–33.5), and the oceanic Kuroshio water (salinity > 33.5). We use these definitions in Figure 4 (and thereafter) to relate seasonal variations in nutrient and TChl *a* concentrations for the three water mass types.

As expected for factors that directly affect phytoplankton growth and biomass accumulation, the spatial variations of nutrient concentrations are generally consistent with the distributions of TChl *a*, with a clear decreasing trend from the coastal river plume to the offshore Kuroshio region (Figure 4A, B). Mean surface concentrations of NO<sub>x</sub> in all these water masses are significantly higher in winter than during summer (Table 3; Figure 4A). Due to strong vertical mixing in winter, MLD are much deeper in the Kuroshio waters (mean ± SD = 68 ± 28 m, *n* = 57) in the winter than in the summer (15 ± 7 m, *n* = 34). Seasonal variations of other nutrients concentrations are similar to that of NO<sub>x</sub>, but the ratios of NO<sub>x</sub>/SRP indicate a pronounced downward trend from the river plume (>60) to the Kuroshio water (<5) during spring and summer (Figure 4C; Table 3). In addition, Si(OH)<sub>4</sub>/NO<sub>x</sub> ratios for the entire study area during spring and summer (>10) are significantly higher than those in autumn and winter (~1.6, Figure 4D; Table 3). Consistent with results from satellite remote sensing, cruise measurements of TChl *a* con-

centrations are highest in the river plume and decline in the Kuroshio water (Figure 4B). For the entire study area, the TChl *a* concentrations in spring and summer are significantly higher than those during autumn and winter (Table 3).

## Phytoplankton Biomass and Community Structure

Based on CHEMTAX analysis, diatoms typically dominate the phytoplankton community of the East China Sea, accounting for an average of 52% of surface TChl *a* values (Figures 5, 6). However, during springtime, the contributions of dinoflagellates to TChl *a* exceed those for diatoms, on average, for the mid-shelf region, and particularly in the river plume (Figures 5A, 6A, B). For these areas, the seasonal shifts from dinoflagellates in spring to diatoms are evident in comparisons of raw values of diagnostic pigments—peridinin (Peri) and fucoxanthin (Fuco), respectively (Figure 7).

At the offshore stations, the importance of larger phytoplankton, diatoms, and/or dinoflagellates, decreases appreciably, and their contributions are partially replaced by cryptophytes, *Synechococcus*, chrysophytes, prymnesiophytes, and *Prochlorococcus* (Figures 5, 6). Biomass of *Prochlorococcus*, as represented by the pigment divinyl-chlorophyll *a* (DV-Chl *a*), is significantly higher in the Kuroshio water than in the river plume, where only trace concentrations are detected during the warm seasons (Figure 8A). In contrast, the maximum concentration of *Synechococcus* is observed in the river plume area during summer (Figure 8B). Relative contributions of chrysophytes (~17%) and prasinophytes (~15%) to TChl *a* are higher in the Kuroshio water during autumn and winter than in

**Table 2.** Definitions of Water Masses in the East China Sea, with Comparison of Dominant Phytoplankton Groups During Spring, Summer, and Late Autumn/Winter Seasons

Water masses	Definition	Spring	Summer	Late autumn/winter
Plume	Salinity < 31	Dinoflagellates Diatoms	Diatoms	Diatoms Cryptophytes Prasinophytes
Mid-shelf water	31 < Salinity < 33.5	Diatoms Dinoflagellates	Diatoms <i>Synechococcus</i> Prasinophytes	Diatoms Cryptophytes Prasinophytes
Kuroshio water	33.5 < Salinity	Diatoms <i>Synechococcus</i> Cryptophytes	Diatoms <i>Synechococcus</i> <i>Prochlorococcus</i>	Diatoms Chrysophytes Prasinophytes

Salinity ranges are measured values in surface (≤ 5 m) waters. Water masses are the river plume (salinity = <31), mid-shelf (salinity = 31–33.5), and Kuroshio waters (salinity > 33.5).

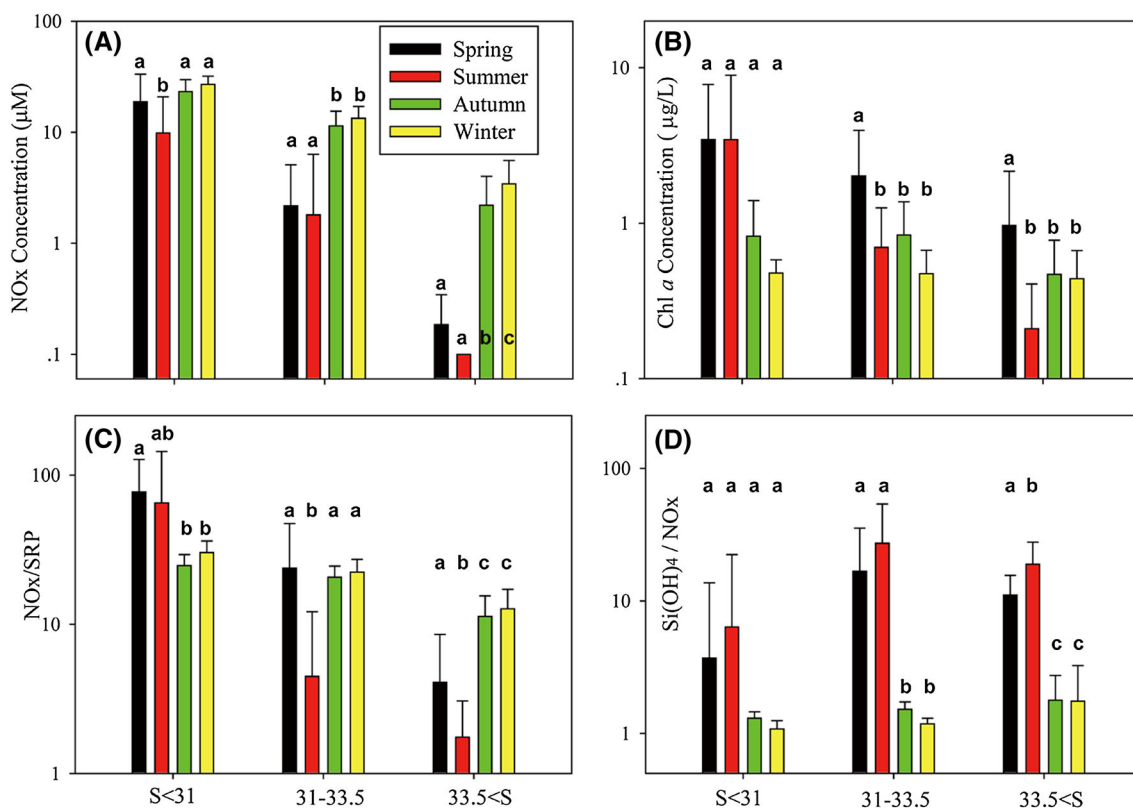


**Figure 4.** Seasonal variations of nitrite plus nitrate ( $\text{NO}_x$ ,  $\mu\text{M}$ ), total chlorophyll *a* concentrations (Tchl *a*,  $\mu\text{g l}^{-1}$ ), and nutrients ratios ( $\text{NO}_x/\text{SRP}$  and  $\text{Si(OH)}_4/\text{NO}_x$ ) in different water masses during four seasons in the East China Sea. Lower case letters in each panel indicate whether seasonal means are significantly different or statistically similar (Table 3).

spring and summer (Figure 6), and cryptophytes are also relatively more important ( $\sim 20\%$  of Tchl *a*) during the cold seasons (Figure 6).

Overall, three seasonal patterns of phytoplankton biomass and community composition in the East China Sea emerge from the CHEMTAX analysis: (i) the spring pattern, with algal blooms in the river plume with high biomass of dinoflagellates and diatoms; (ii) the summer and early autumn pattern, with significant spatial differences, including high biomass of diatoms in the river plume and low biomass and picophytoplankton dominance in the Kuroshio water; and (iii) the late autumn and winter pattern, with relatively low biomass and uniform distributions but higher contributions of cryptophytes, prasinophytes, and chrysophytes (Figures 5, 6; Table 2).

### Statistical and Model Analyses

We performed Canonical Correspondence Analyses (CCA) on major pigments separately for the four seasons (Figure 9). The suites of environmental parameters explain 35–62% variability of phytoplankton communities in different seasons. In

general, nutrients group closely together with Tchl *a*, while temperature, salinity, MLD, and station depth align in the opposite direction (Figure 9). In springtime, diatom and dinoflagellates are close to Tchl *a*, suggesting the dominance of diatoms and/or dinoflagellates when Tchl *a* is elevated. However, dinoflagellates extend more on that dimension indicating a stronger correlation (Figure 9A). In summer, the broader dominance of diatoms (and prasinophytes and cryptophytes) in high-nutrient and bloom areas is indicated by the tight packing of their with Tchl *a* and major nutrients, while dinoflagellates are relatively far from these factors (Figure 9B). *Prochlorococcus* remains closely aligned with bottom depth (temperature and salinity as well) throughout the year, indicating a close relationship with the Kuroshio waters (Figure 9B). However, *Synechococcus* notably resides apart from *Prochlorococcus* and close to chlorophytes, prasinophytes, chrysophytes, and prymnesiophytes.

In our GAMs, month, temperature, salinity, and  $\text{NO}_x$  concentrations are strong predictors of the concentrations of diatoms, dinoflagellates, *Synechococcus*, and *Prochlorococcus* (Figure 10, all

**Table 3.** Summary of Means and Standard Deviations (SD) of Nitrate + Nitrite ( $\text{NO}_x$ ), Total Chlorophyll *a* (TChl *a*) Concentrations, and Nutrient Ratios ( $\text{NO}_x/\text{Soluble Reactive Phosphate}$  and  $\text{Si(OH)}_4/\text{NO}_x$ ) in the Surface Water of the Entire Study Area and Different Water Masses (Table 2)

	$\text{NO}_x$			TChl <i>a</i>			$\text{NO}_x/\text{SRP}$			$\text{Si(OH)}_4/\text{NO}_x$						
	S	A	W	S	S	A	W	S	S	A	W	S	S	A	W	
	<i>P</i> = 0.00			<i>P</i> = 0.00			<i>F</i> = 9.63			<i>P</i> = 0.01			<i>P</i> = 0.00			
Total																
Mean	5.04	4.62	6.40	8.62	2.10	1.94	0.58	0.45	29.15	29.39	14.71	17.02	12.42	16.06	1.67	1.55
SD	9.85	8.65	7.69	8.91	2.77	4.13	0.42	0.21	38.29	59.52	6.62	8.08	15.00	19.87	0.82	1.25
	<i>F</i> = 3.17			<i>F</i> = 9.63			<i>F</i> = 9.63			<i>F</i> = 4.32			<i>F</i> = 29.27			
<i>S</i> < 31																
Mean	18.80	9.83	23.20	26.94	3.45	3.44	0.82	0.48	77.09	65.21	24.78	30.27	3.70	6.35	1.30	1.08
SD	14.58	11.04	6.55	5.11	4.34	5.50	0.57	0.10	50.42	78.93	4.57	5.97	9.99	15.99	0.15	0.17
	<i>F</i> = 7.49			<i>F</i> = 0.12			<i>F</i> = 1.98			<i>F</i> = 2.89			<i>F</i> = 0.51			
31–33.5																
Mean	2.17	1.80	11.38	13.36	2.01	0.70	0.84	0.47	23.78	4.48	20.72	22.43	16.75	27.27	1.52	1.18
SD	2.92	4.52	4.07	3.74	1.94	0.56	0.53	0.19	23.63	7.68	3.87	4.86	18.63	26.59	0.21	0.12
	<i>F</i> = 58.26			<i>P</i> = 0.00			<i>F</i> = 11.25			<i>P</i> = 0.00			<i>P</i> = 0.00			
<i>S</i> > 33.5																
Mean	0.19	0.10	2.21	3.43	0.97	0.21	0.47	0.44	4.09	1.75	11.32	12.71	11.08	18.91	1.78	1.75
SD	0.16	0.00	1.80	2.13	1.19	0.20	0.31	0.23	4.48	1.32	4.20	4.45	4.49	8.87	0.96	1.49
	<i>F</i> = 29.72			<i>P</i> = 0.00			<i>F</i> = 10.86			<i>P</i> = 0.00			<i>F</i> = 46.01			

The *F* and *P* values in one-way ANOVA indicate significant differences among seasons. Seasons (S, S, A, W) are arranged in order of spring, summer, autumn and winter. Nutrients values are for surface water samples for cruises C1–C4 and E1–E3 only, and TChl *a* values are surface concentrations from all cruises.



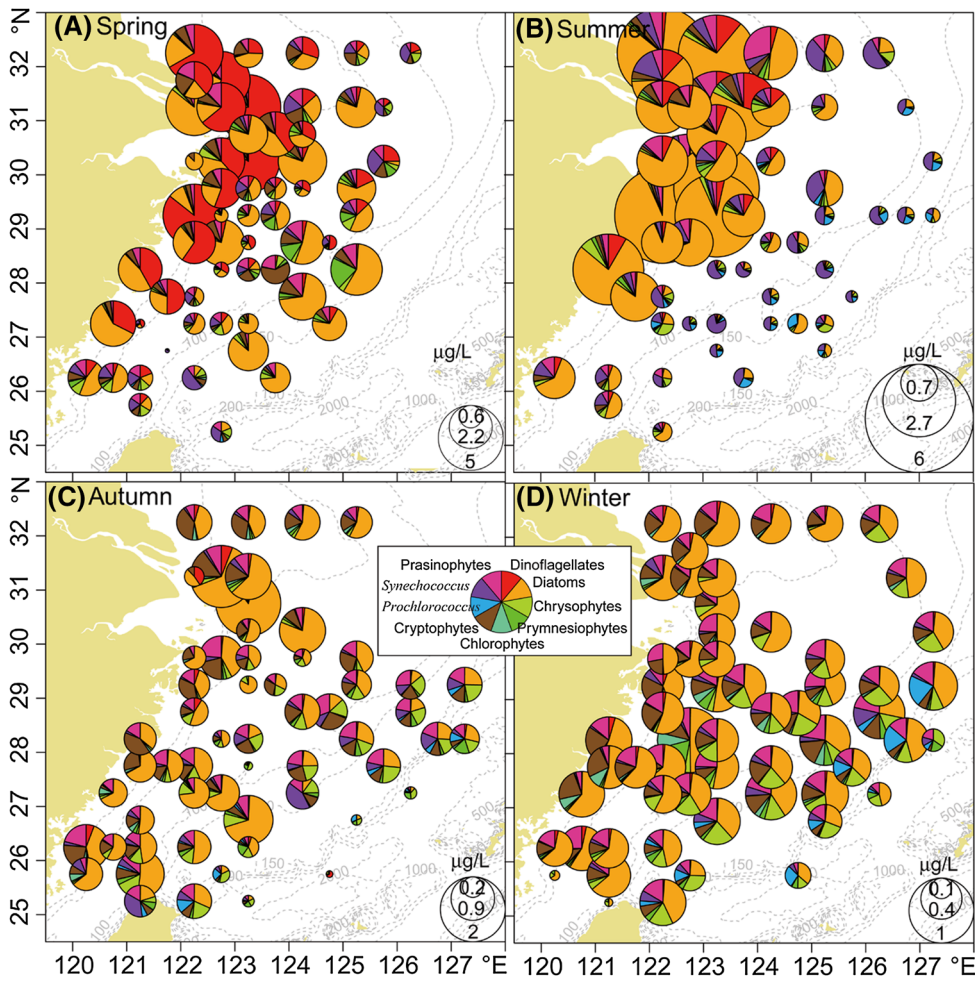


Figure 5. Seasonal distributions of phytoplankton community biomass and composition in surface water samples from 11 cruises in the East China Sea from 2006 to 2012 (Table 1). Pie graph diameter is proportional to the mean total chlorophyll *a* (TChl *a*), and composition reflects the contributions of different phytoplankton groups to TChl *a* determined from CHEMTAX assessment of diagnostic pigments. All data are averaged over  $0.5^{\circ} \times 0.5^{\circ}$  grid boxes.

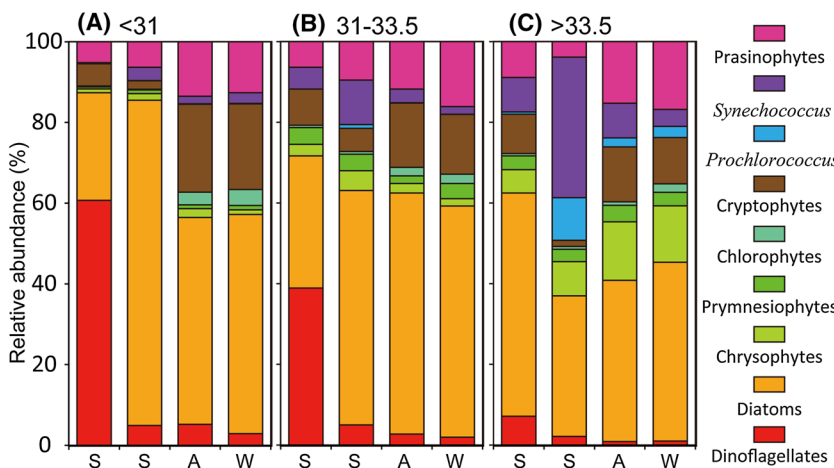
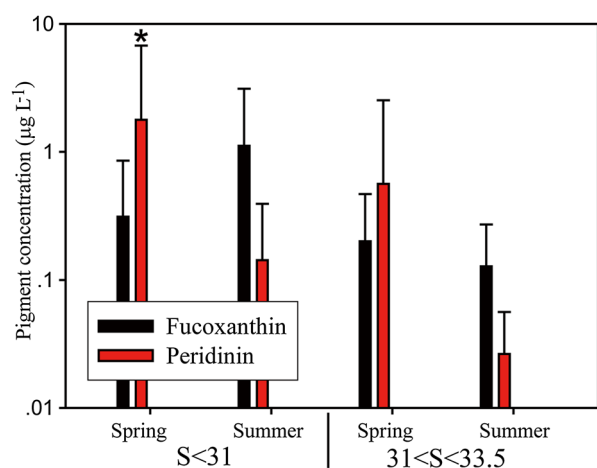


Figure 6. Seasonal variations of the contributions of different phytoplankton groups to total chlorophyll *a* (%) in the three water masses (A–C) in the East China Sea. Compositions are determined from CHEMTAX assessment of diagnostic pigments. Seasons (S, S, A, W) are arranged in order of spring, summer, autumn, and winter.

$P < 0.05$ ). The effects of month on the concentrations of diatoms and dinoflagellates clearly show the differences in their seasonal variations, with a broad peak for diatoms in spring and summer and a more pronounced but narrower peak for dinoflagellates in late spring and early summer (Figure 10A). The effect of temperature on

dinoflagellates is pronounced, in contrast to the only summer temperature optimum ( $\sim 26^{\circ}\text{C}$ ) for diatoms (Figure 10B). In addition, there is a clear mid-range salinity optimum ( $\sim 31$ ) for dinoflagellates, whereas the correlation between salinity and diatoms is monotonically negative (Figure 10C). Furthermore, while diatoms benefit clearly from



**Figure 7.** Mean and standard deviation of surface sea water concentrations of fucoxanthin and peridinin during spring and summer seasons in river plume ( $S < 31$ ) and mid-shelf waters ( $31 < S < 31.5$ ) in the East China Sea. Asterisk indicates significant difference.

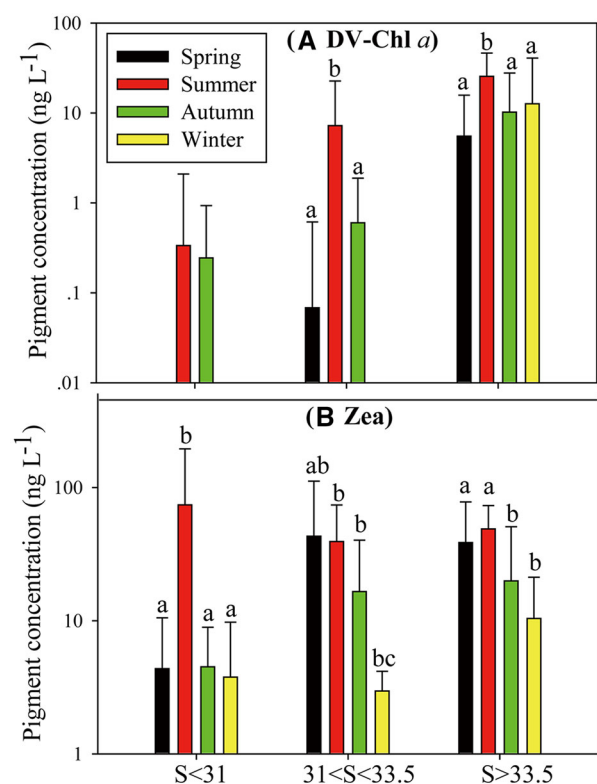


**Figure 8.** Seasonal variations of mean surface concentrations and standard deviation of divinyl-chlorophyll *a* (A, DV-Chl *a*) and Zeaxanthin (B, Zea) in different water masses in the East China Sea. Lower case letters in each panel indicate whether seasonal means are significantly different or statistically similar.

increasing nutrients over the full range of measured concentrations, the more complicated dinoflagellate response suggests optimal conditions at intermediate  $\text{NO}_x$  concentrations (Figure 10D).

Similar seasonal patterns of *Synechococcus* and *Prochlorococcus* are observed in the GAMs results, both with broad maxima in the summer and autumn, and with generally strong positive relationships to increasing temperature (Figure 10E, F). However, there is a time lag between the increases of *Synechococcus* and *Prochlorococcus* during the warm seasons, with *Synechococcus* leading and *Prochlorococcus* increasing rapidly after temperatures reach  $18^\circ\text{C}$  (Figure 10F). Moreover, *Prochlorococcus* responds rapidly to increasing salinity above 31, while salinity has a relatively modest impact on *Synechococcus* (Figure 10G). Similarly, *Prochlorococcus* declines rapidly as nutrients increase, while the decrease of *Synechococcus* is more gradual (Figure 10H).

## DISCUSSION

### Driving Mechanisms of Seasonal Variability in the East China Sea

The seasonal fluctuations of several water masses make the East China Sea shelf a highly dynamic region (Ning and others 1998; Gong and others 2003) with variable seasonal patterns of phytoplankton biomass (Chl *a*) among its subareas (Yamaguchi and others 2012). Low temperature, strong winds, and vigorous vertical mixing during the Northeast Monsoon deepen the MLD, providing abundant nutrients for phytoplankton (Figure 4), but further reducing the mean light level experienced in the euphotic zone (Gong and others 2003). Therefore, due to light limitation and possibly low-temperature effects on phytoplankton growth, TChl *a* values remain generally low over the entire study area during winter (Table 3). During the summer, prevailing winds from the Southwest Monsoon drive upwelling on the East China Sea, leading to increased nutrient concentrations and phytoplankton blooms along the coast (Ning and others 1998; Furuya and others 2003; Tang and others 2006). These winds also cause the Changjiang River plume, with its very high  $\text{NO}_x$  loading but relative low  $\text{PO}_4^{3-}$  concentrations (Figure 4), to shift from the river mouth to the broader continental shelf from July to September (Gong and others 2003; Yamaguchi and others 2012). Thus, the East China Sea coastal waters receive abundant nutrients from both river and upwelling sources during the summer (Gong and others

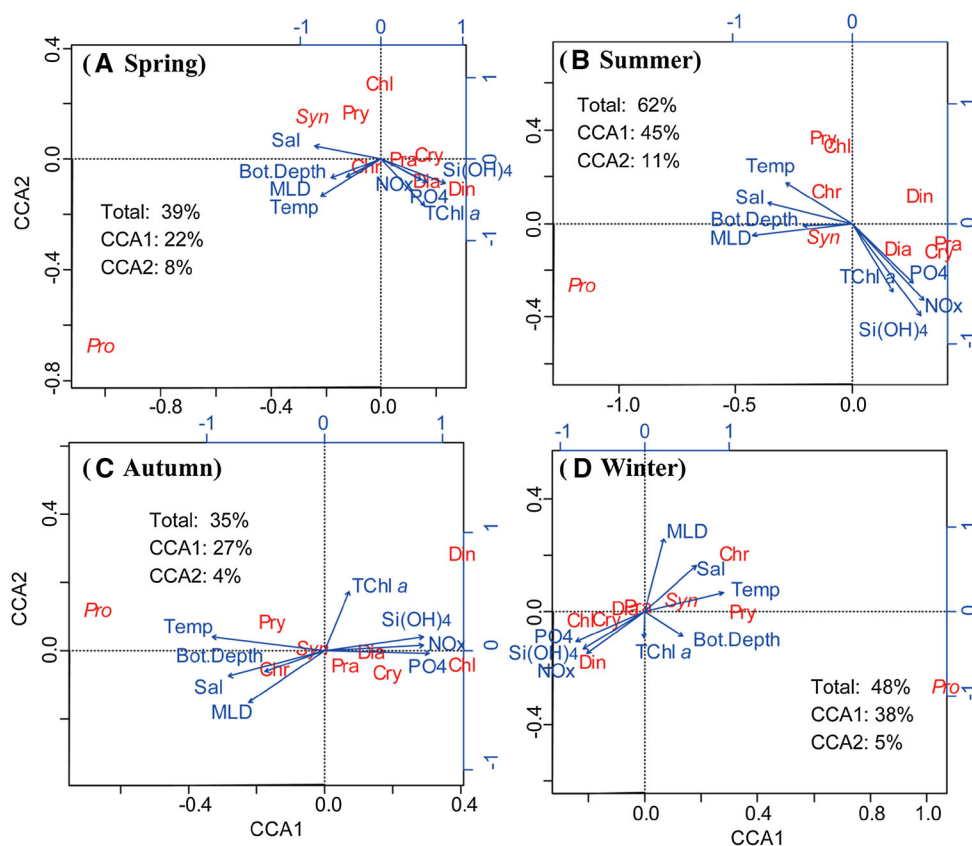


**Figure 9.** Canonical correspondence analyses (CCA) of the seasonal relationships between phytoplankton chlorophyll *a* concentrations (red letters) and environmental factors (blue arrows) in the East China Sea. Blue axes on the top and right are for sea surface values of environmental factors, while axes on the bottom and left are surface values for phytoplankton. Percentages indicate the variability of phytoplankton explained by all environmental factors (Total) or by dimensions 1 (CCA1) and 2 (CCA2). Variable are: temperature (Temp), salinity (Sal), bottom depth (Bot.Depth), nitrate + nitrite (NO<sub>x</sub>), phosphate (PO<sub>4</sub>), Si(OH)<sub>4</sub>, total chlorophyll *a* (TChl *a*), diatoms (Dia), dinoflagellates (Din), chrysophytes (Chr), chlorophytes (Chl), prasinophytes (Pra), prymnesiophytes (Pry), cryptophytes (Cry), *Synechococcus* (Syn), and *Prochlorococcus* (Pro) (Color figure online).

1996), which enhance phytoplankton biomass and production (Gong and others 2011). Primary production over the shelf in summer is 939 mg C m<sup>-2</sup> day<sup>-1</sup> on average, about three times higher than the rates measured in other seasons (Gong and others 2003).

Although not evident in primary production, mean surface TChl *a* values for the entire East China Sea shelf are higher in spring than summer (Figures 3, 4, Yamaguchi and others 2013), due to blooms that utilize the residual nutrients in surface waters from winter mixing (Furuya and others 2003). In addition, increased nutrient loading from anthropogenic activities in China has resulted in an increasing late-spring trend in phytoplankton standing stock in 1984–2002 in the Changjiang River estuary and adjacent coastal area (Zhou and others 2008; Jiang and others 2014). Generally speaking, therefore, TChl *a* biomass over the shelf is

higher in spring than summer, especially away from the river plume (Figure 4B), and this seasonal difference appears to be increasing.

The mismatch between primary productivity and TChl *a* biomass seems to result from photo acclimation, as recently suggested by Behrenfeld and others (2015), and also from the top-down effects. Although the TChl *a* concentration during spring is higher, the temporal variation on phytoplankton carbon biomass may not be the case as the light-driven (photo acclimation) and nutrient-driven physiological responses (Behrenfeld and others 2015). Indeed, variations of the phytoplankton carbon-to-chlorophyll *a* ratio in the East China Sea are significant (Chang and others 2003). On the other hand, previous study has indicated that phytoplankton standing stock is controlled more by the microzooplankton in summer (Zheng and others 2015). The mean rates of microzooplankton

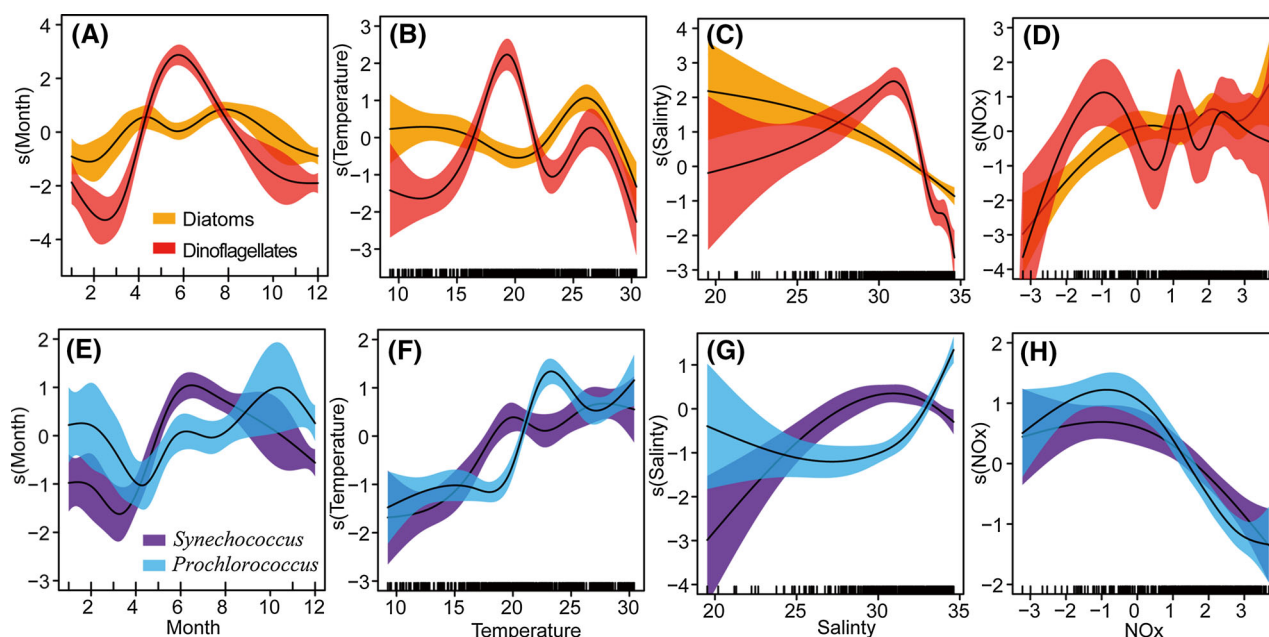


**Figure 10.** Results of Generalized Additive Models (GAMs) describing the chlorophyll *a* variability of four phytoplankton groups (diatoms, dinoflagellates, *Synechococcus*, and *Prochlorococcus*) with month (**A**, **E**), temperature ( $^{\circ}\text{C}$ ; **B**, **F**), salinity (**C**, **G**), and nitrate + nitrite concentration ( $\text{NO}_x$ ; **D**, **H**) in the East China Sea. Concentrations of phytoplankton Chl *a* ( $\text{ng l}^{-1}$ ) and  $\text{NO}_x$  ( $\mu\text{M}$ ) are natural logarithm transformed and are plotted as differences between concentrations and mean values. *Solid lines* represent smoothed mean relationships from GAMs, and *shaded areas* are 95% confidence intervals. The *inward tick marks* on the *horizontal axes* show data distributions.

grazing rate ( $0.93 \pm 0.41 \text{ day}^{-1}$ ) and pressure ( $\text{m } \mu^{-1}$ ,  $\sim 60\%$ ) in summer were significantly higher than those in winter ( $0.25 \pm 0.08 \text{ day}^{-1}$ ,  $\sim 22\%$ ) (Zheng and others 2015). In addition to the relatively low temperature during spring, communities dominated by dinoflagellates might be another explanation for the low grazing pressures. Due to lack of sufficient data, we did not take into account the photo acclimation and top-down effects in our models. In addition, autumn is not well represented in our dataset, which lacks cruise data between 27 August and 26 November (Table 1). Very likely, however, the moderately stratified water and high-nutrient levels in the coastal area during autumn promote diatom blooms (Figure 3C).

### Niche Differentiation of Major Phytoplankton Groups in the East China Sea

To confirm the phytoplankton compositional assessments based on pigments, we compared the concentrations of dominant groups from CHEMTAX calculations to published results from microscopic and flow cytometric analyses for cruises C1-C4 (Guo and others 2014a, b). Because of the high

specificity of diagnostic pigments for *Prochlorococcus* (DV-Chl *a*) and *Synechococcus* (Zea), the comparisons between HPLC-CHEMTAX and these flow cytometry determined populations are especially good (Figure 11, higher  $R^2$ ). Nonetheless, adequate correlations are also observed between pigment and microscopy-based biomass assessments of larger taxa, including diatoms and dinoflagellates (Figure 11, all  $P < 0.01$ ), and similar results were reported in the Yellow Sea (Liu and others 2015a). The HPLC-CHEMTAX approach is particularly well suited for discriminating groups of intermediate-sized phytoplankton, such as chrysophytes, chlorophytes, prasinophytes, and prymnesiophytes, that cannot be easily identified by microscopy or flow cytometric methods (Goela and others 2014).

#### *Diatom and Dinoflagellates*

Our GAMs show that diatoms occur over a relatively wide temperature range in the East China Sea, and only decline in biomass at temperatures above  $26^{\circ}\text{C}$ . Seasonal peaks in diatoms (Figure 10A) are associated with phytoplankton blooms in early spring (relatively low temperature) and in the river plume during summer (high tem-



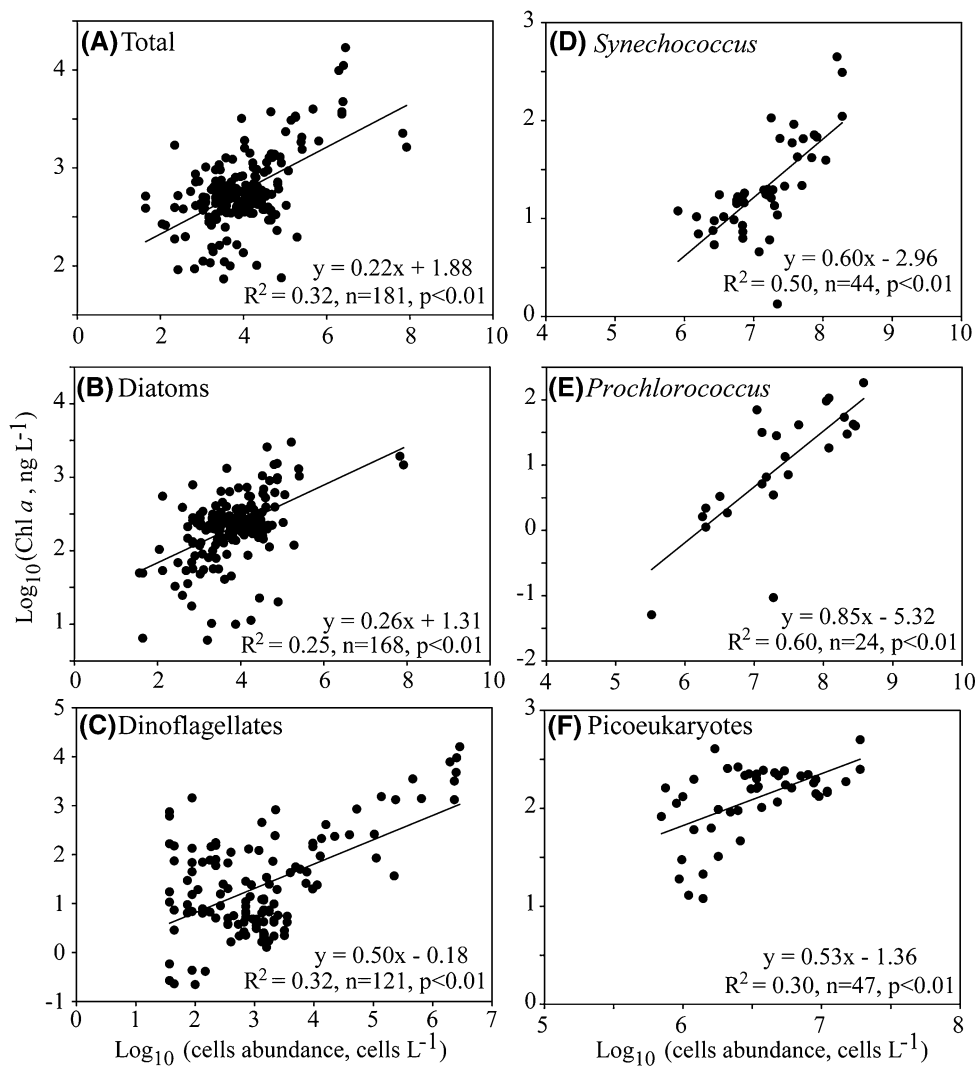


**Figure 11.** Comparison of the results between chlorophyll *a* concentration using HPLC-CHEMTAX analyses and cells abundances using microscopic and flow cytometry observations for cruises C1-C4. For the total cells (A), diatoms (B), and dinoflagellates (C), the chlorophyll *a* concentrations and cells numbers are obtained from HPLC-CHEMTAX and microscopic analyses, respectively. For *Synechococcus* (E), *Prochlorococcus* (F), and picoeukaryotes (G), chlorophyll *a* biomass and abundance are obtained from HPLC-CHEMTAX and flow cytometry analyses, respectively. Chlorophyll *a* concentrations of picoeukaryotes using CHEMTAX are the sum of chrysophytes, chlorophytes, prasinophytes, prymnesiophytes, and cryptophytes.

perature). The dominant species in the East China Sea are mostly chain-forming diatoms, with *Pseudo-nitzschia delicatissima*, *Thalassionema nitzschioides*, and *Paralia sulcata* being the most common over the 4 seasons (Guo and others 2014b). Based on laboratory studies, marine diatoms have significantly higher maximum carbon-specific nutrient uptake rates compared to other groups, and they are notably strong competitors for nitrate (Litchman and others 2007). Small diatoms typically exhibit a “velocity” strategy, with high maximum rates of nutrient uptake and growth, whereas large diatoms tend to be more “storage adapted,” with disproportionately large storage vacuoles (Sommer 1984; Litchman and others 2007). Thus, diatoms as a group have varying advantages that contribute to their relative success under conditions of both high and fluctuating nutrients (Table 2).

Nonetheless, during springtime, concentrations of Peri are significantly higher than other diag-

nostic pigments in the river plume area, and they are comparable to Fuco concentrations in mid-shelf waters as well (Figure 7). We take these as conservative indications of the relative importance of dinoflagellates during these times, given that the specificity of Peri to dinoflagellates is higher than that of Fuco to diatoms, and the ratios of Peri to TChl *a* are usually less than those of Fuco:Chl *a* (Higgins and others 2011). Thus, dinoflagellate biomass in the spring may be higher overall than biomass of diatoms (Figures 5, 6; Table 2). Indeed, the CCA shows a seasonal shift in proximity of dinoflagellate and diatoms to TChl *a* from spring to summer (Figure 9), with dinoflagellates most closely aligned with TChl *a* in spring and diatoms in summer. The dominant dinoflagellate in spring is *Prorocentrum dentatum* (renamed *Prorocentrum donghaiense* Lu), and *Scrippsiella trochoidea* and *Gymnodinium lohmanni* are also relatively abundant (Guo and others 2014b). Based on long-term observa-

tions, the contribution of diatoms in the Changjiang River estuary and adjacent coastal waters has decreased from about 85% of TChl *a* in 1984 to about 60% in 2000 (Zhou and others 2008). Over the same time, red tide and harmful algal blooms have increased dramatically in terms of both number and scale (Zhou and others 2008). Various abilities of dinoflagellates to migrate and exploit shallow nutriclines, to utilize organic phosphorus compounds via alkaline phosphatase, and to feed mixotrophically allow them to persist under conditions unfavorable for diatoms (Litchman and others 2007). Our GAMs suggest that dinoflagellates have a relative advantage over diatoms at lower nutrient concentrations (Figure 10D). In addition, with a decline of Si:N from 1.5 to 0.4 following construction of the Three Gorges Dam in 2003, it appears that diatoms might further decline in the plume due to the unfavorable change in nutrient ratio (Gong and others 2006). However, we believe that the Si(OH)<sub>4</sub> in this system is rich overall (Figure 4D) and that the impact of NO<sub>x</sub>/SRP on the relative abundance of dinoflagellates to diatoms may be more important. During cruise C1, we usually observed dinoflagellate blooms (Figure 11C, exceeding 10<sup>6</sup> cells l<sup>-1</sup>) in the surface coastal area with high Si(OH)<sub>4</sub> (> 10 μM) but quite low SRP concentrations (below the detection limit). There is a clear shift for the study area from being potential *P*-limited in river plume to *N*-limited in the Kuroshio water (Figure 4C, D). Additional studies in the East China Sea have also suggested that the increase of N:P ratio in the coastal area could well be the key cause of the shift from diatom to dinoflagellate dominance (Zhou and others 2008; Guo and others 2014b; Jiang and others 2014). The ongoing decrease in the ratio of diatoms to dinoflagellates in the East China Sea, and the associated problem of increasing harmful algal blooms, appear to be closely related to increasing anthropogenic activities and climatic change influences in the region (Zhou and others 2008; Jiang and others 2014).

Using long-term data of 66 plankton taxa collected over the period from 1958 to 2002 in the North Sea, Edwards and Richardson (2004) found that the timing of seasonal peaks of dinoflagellates have moved significantly forward (principally, the genera *Ceratium* by 27 days, *Protoperidinium* by 26 days, and *Dinophysis* by 24 days), whereas diatom peaks in spring and autumn have collectively remained static, albeit with considerable taxon-specific variation. Our GAM analyses show strong relationships between bloom timing (month) and temperature for dinoflagellates (Figure 10). In

contrast, the peaks are broader and more gentle for diatoms, implying less temperature sensitivity for diatoms (Figure 10), which is consistent with previous speculation that diatoms may be more dependent on day length or light intensity rather than on temperature-mediated physiology (Edwards and Richardson 2004). Therefore, temperature (and N/P) or light, which increases first during spring blooms, might determine their competitive results. Similar results have been found recently at a time series station in the western English Channel using a 14-year dataset (Xie and others 2015). Both recent trends, as well as consideration of future changes, therefore, suggest a more important role of dinoflagellates in the East China Sea ecosystem, including a change in timing and higher relative abundances of springtime blooms.

#### *Prochlorococcus and Synechococcus*

Photosynthetic bacteria, like *Prochlorococcus* and *Synechococcus*, are typical dominants in low-latitude open-ocean ecosystems (Zwirgmaier and others 2008), under conditions of higher surface irradiance, warmer temperature, enhanced water-column stratification, and oligotrophy. It is not clear, however, whether direct or indirect (stratification, low nutrients) effects of temperature lead primarily to their success (Chen and others 2014), because temperature and nutrients are often negatively correlated in the ocean.

Our results show a relatively close relationship between *Synechococcus* and nutrients (Figures 9, 10H), with the highest biomass in the river plume (Figure 8B). According to Guo and others (2014a), mean abundance of *Synechococcus* is also higher in summer ( $7.6 \times 10^4$  cells ml<sup>-1</sup>, range  $7.0 \times 10^3$ – $3.8 \times 10^5$  cells ml<sup>-1</sup>) than in winter ( $1.0 \times 10^4$  cells ml<sup>-1</sup>, range  $<0.1$ – $9.1 \times 10^4$  cells ml<sup>-1</sup>), as well as significantly higher in the surface plume waters than the mid-shelf ( $P < 0.01$ ) and Kuroshio ( $P < 0.05$ ) regions in summer. In contrast, *Prochlorococcus* abundance is low in river-influenced waters (Figure 8A), regardless of temperature and nutrients there (Figure 10; Guo and others 2014a, b). Jiao and others (2005) also found that *Prochlorococcus* are largely confined to the warm water current areas and almost absent in the coastal areas in the winter. They suggested that the lower boundaries of temperature and salinity for abundant *Prochlorococcus* in surface waters are around 15.6, 33.5°C respectively, in winter and 26.4 versus 29.1°C, respectively, in summer (Jiao and others 2005). Our GAMs model shows similar

distributional ranges of temperature and salinity (Figure 10).

At temperatures above 18°C, both *Synechococcus* and *Prochlorococcus* correlate positively with temperature (Figure 10F). However, salinity has a more pronounced impact on *Prochlorococcus* than on *Synechococcus* (Figure 10G). In addition, the different trends of *Prochlorococcus* and *Synechococcus* with  $\text{NO}_x$  when  $\text{NO}_x$  is very low but increasing suggest a strong advantage for *Synechococcus* in oligotrophic waters of improving nutrient status (Figure 10H). Chung and others (2011) have also revealed that enhancements of nutrient concentrations from Asian dust storms stimulate rapid growth of *Synechococcus* in the Kuroshio Current, whereas abundances of *Prochlorococcus* either remained unaffected or declined modestly. Zwiirglmaier and others (2008) reported that 40.7% of the variance for *Prochlorococcus* globally, can be explained by the physical parameters of temperature light and depth, whereas nutrients ( $\text{PO}_4^{3-}$ ,  $\text{NO}_2^-$ , and  $\text{NO}_3^-$ ) account for 22.4% of the variance of *Synechococcus*. Indeed, temperature or salinity is implicated as key ecological determinants for *Prochlorococcus* community structure in a variety of laboratory, basin-, and global-scale studies (Zwiirglmaier and others 2008). In contrast, *Synechococcus* is observed in warm and salty waters, as well as environments with low salinities and (or) low temperatures (Partensky and others 1999; Flombaum and others 2013).

Our results support the idea that *Prochlorococcus* will benefit more than *Synechococcus* from higher temperature, increased stratification and lower nutrients expected from global warming. However, our CCA and GAMs were constructed to fit field data on biomass rather than growth rate potential, the results reflect net differences in the trophic interactions of photosynthetic bacteria as well as their physiological responses (Zwiirglmaier and others 2008). Guo and others (2014a) found that protistan grazers in the East China Sea consumed 84 and 79% of *Prochlorococcus* and *Synechococcus* production, respectively, in summer and 45 versus 47%, respectively, in winter. These two taxa therefore have roughly comparable vulnerabilities to small predators, and both suffer disproportionate losses to grazers at higher temperature. Since heterotrophic processes, including zooplankton grazing, may generally have the potential to increase faster with temperature than phytoplankton growth and production (Chen and others 2012), increased losses to grazing with climate warming could set lower summertime abundances of *Prochlorococcus* and *Synechococcus* in the East China Sea.

### Other Phytoplankton Groups

In addition to the above four major groups, our results indicate that chrysophytes, prasinophytes, and cryptophytes achieve considerable biomass and relative contributions to TChl *a* in the East China Sea, especially during the cold seasons (Figures 5, 6; Table 2). Based on CCA analysis, the niche spaces for these groups are mainly located between *Prochlorococcus* and larger phytoplankton (diatom and dinoflagellates) (Figure 9). Together, therefore, this taxonomically complex assemblage of pico- and nano-sized phytoplankton conforms to the general perception of a broad structuring role of cell size in phytoplankton community composition (Litchman and others 2007). Although these intermediate groups are poorly investigated in the East China Sea, as in most systems, recent studies using *in situ* hybridization with 18S rRNA-specific probes have revealed spring blooms of haptophytes reaching  $2.2 \times 10^4$  cells  $\text{ml}^{-1}$ , as well as higher haptophyte contributions to nanoflagellate abundance in spring (32%) than in summer (12%) months (Lin and others 2014). Small-sized eukaryotic phytoplankton, including haptophytes and prasinophytes, have also been identified in several studies as mixotrophs and major predators of prokaryote cells (Zubkov and Tarran 2008; McKie-Krisberg and Sanders 2014), which expands their niche possibilities and trophic importance in pelagic food webs (Mitra and others 2014). Future studies in the East China Sea should look in more detail at the distributions and responses of these groups.

## CONCLUSIONS

The present study synthesizes current knowledge of phytoplankton biomass and community structure for the continental shelf area and four seasons in the East China Sea. The combination of long-term satellite imagery, direct field observations measurements, and CCA and GAMs reveal three seasonal patterns (Table 2). During winter, TChl *a* values remain low despite rich nutrients, with the growth of phytoplankton limited mainly by light availability. In summer, extremely large spatial variations of TChl *a* biomass and community composition are observed. In addition, high TChl *a* concentrations occur over the continental shelf during spring and summer, with generally higher values in the spring. We suggest that a more important role for dinoflagellates in the future East China Sea. The influences of nutrient ratios (especially N:P) may be very important in regulat-

ing the relative abundance of dinoflagellates to diatoms. In addition, physical parameters (temperature and salinity) and chemical parameters (nutrients) are relatively more critical for *Prochlorococcus* and for *Synechococcus*, respectively. Additional groups, chrysophytes, prasinophytes, and cryptophytes, contribute significantly to biomass and TChl *a*, especially during winter. Future studies in the East China Sea should look at the distribution and responses of these small-sized eukaryotic phytoplankton groups.

## ACKNOWLEDGEMENTS

This work was supported by Grants from the China NSF (Nos. 41330961, U1406403, 41406143, and 41176112), the National Basic Research Programme (Nos. 2015CB954002, 2011CB403603), and the Chinese Academy of Science project (XDA11020103). We thank Professor Caiyun Zhang of Xiamen University for her help to obtain and analyze satellites data and Professor John Hodgkiss of The University of Hong Kong for his English language editing and comments on the manuscript. We thank Professors Daji Huang, Jianyu Hu, and Hao Wei for providing hydrographic data and Professors Minhan Dai and Sumei Liu for providing inorganic nutrient data. We would like to thank the captains and crew of the R/V "Beidou" and "Dongfanghong 2," who made concerted efforts to assist during field sampling. We do appreciate the comments and suggestion on the manuscript from anonymous reviewers.

## REFERENCES

- Anderson DM, Cembella AD, Hallegraeff GM. 2012. Progress in understanding harmful algal blooms: paradigm shifts and new technologies for research, monitoring, and management. *Annu Rev Mar Sci* 4:143–76.
- Bakun A. 1990. Global climate change and intensification of coastal ocean upwelling. *Science* 247:198–201.
- Behrenfeld M. 2011. Uncertain future for ocean algae. *Nat Clim Chang* 1:33–4.
- Behrenfeld MJ, O'Malley RT, Boss ES, Westberry TK, Graff JR, Halsey KH, Milligan AJ, Siegel DA, Brown MB. 2015. Reevaluating ocean warming impacts on global phytoplankton. *Nat Clim Chang*. doi:10.1038/nclimate2838.
- Boyce DG, Lewis MR, Worm B. 2010. Global phytoplankton decline over the past century. *Nature* 466:591–6.
- Boyd PW, Lennartz ST, Glover DM, Doney SC. 2015. Biological ramifications of climate-change-mediated oceanic multi-stressors. *Nat Clim Chang* 5:71–9.
- Chang J, Shiah F, Gong G, Chiang K. 2003. Cross-shelf variation in carbon-to-chlorophyll *a* ratios in the East China Sea, summer 1998. *Deep Sea Res Part II* 50:1237–47.
- Chavez FP, Messie M, Pennington JT. 2011. Marine primary production in relation to climate variability and change. *Annu Rev Mar Sci* 3:227–60.
- Chen BZ, Landry MR, Huang BQ, Liu HB. 2012. Does warming enhance the effect of microzooplankton grazing on marine phytoplankton in the ocean? *Limnol Oceanogr* 57:519–26.
- Chen BZ, Liu HB, Huang BQ, Wang J. 2014. Temperature effects on the growth rate of marine picoplankton. *Mar Ecol Prog Ser* 505:37–47.
- Chen CTA. 2009. Chemical and physical fronts in the Bohai, Yellow and East China seas. *J Mar Syst* 78:394–410.
- Chiang KP, Chen YT, Gong GC. 1999. Spring distribution of diatom assemblages in the East China Sea. *Mar Ecol Prog Ser* 186:75–86.
- Chiang KP, Chou YH, Chang J, Gong GC. 2004. Winter distribution of diatom assemblages in the East China Sea. *J Oceanogr* 60:1053–62.
- Chiang KP, Kuo MC, Chang J, Wang RH, Gong GC. 2002. Spatial and temporal variation of the *Synechococcus* population in the East China Sea and its contribution to phytoplankton biomass. *Cont Shelf Res* 22:3–13.
- Chung CC, Chang J, Gong GC, Hsu SC, Chiang KP, Liao CW. 2011. Effects of Asian dust storms on *synechococcus* populations in the subtropical Kuroshio Current. *Mar Biotechnol* 13:751–63.
- Doney SC, Ruckelshaus M, Duffy JE, Barry JP, Chan F, English CA, Galindo HM, Grebmeier JM, Hollowed AB, Knowlton N, Polovina J, Rabalais NN, Sydeman WJ, Talley LD. 2012. Climate change impacts on marine ecosystems. *Annu Rev Mar Sci* 4:11–37.
- Edwards M, Richardson AJ. 2004. Impact of climate change on marine pelagic phenology and trophic mismatch. *Nature* 430:881–4.
- Falkowski PG, Katz ME, Knoll AH, Quigg A, Raven JA, Schofield O, Taylor FJR. 2004. The evolution of modern eukaryotic phytoplankton. *Science* 305:354–60.
- Falkowski PG, Oliver MJ. 2007. Mix and match: how climate selects phytoplankton. *Nat Rev Microbiol* 5:813–19.
- Field CB, Behrenfeld MJ, Randerson JT, Falkowski P. 1998. Primary production of the biosphere: integrating terrestrial and oceanic components. *Science* 281:237–40.
- Flombaum P, Gallegos JL, Gordillo RA, Rincon J, Zabala LL, Jiao N, Karl DM, Li WK, Lomas MW, Veneziano D, Vera CS, Vrugt JA, Martiny AC. 2013. Present and future global distributions of the marine Cyanobacteria *Prochlorococcus* and *Synechococcus*. *Proc Natl Acad Sci USA* 110:9824–9.
- Furuya K, Hayashi M, Yabushita Y, Ishikawa A. 2003. Phytoplankton dynamics in the East China Sea in spring and summer as revealed by HPLC-derived pigment signatures. *Deep Sea Res Part II* 50:367–87.
- Glibert PM, Allen JJ, Artioli Y, Beusen A, Bouwman L, Harle J, Holmes R, Holt J. 2014. Vulnerability of coastal ecosystems to changes in harmful algal bloom distribution in response to climate change: projections based on model analysis. *Glob Chang Biol* 20:3845–58.
- Goela PC, Danchenko S, Icelly JD, Lubian LM, Cristina S, Newton A. 2014. Using CHEMTAX to evaluate seasonal and interannual dynamics of the phytoplankton community off the South-west coast of Portugal. *Estuar Coast Shelf Sci* 151:112–23.
- Gong GC, Chang J, Chiang KP, Hsiung TM, Hung CC, Duan SW, Codispoti LA. 2006. Reduction of primary production and



- changing of nutrient ratio in the East China Sea: effect of the Three Gorges Dam? *Geophys Res Lett* 33:L07610.
- Gong GC, Chen YLL, Liu KK. 1996. Chemical hydrography and chlorophyll *a* distribution in the East China Sea in summer: implications in nutrient dynamics. *Cont Shelf Res* 16:1561–90.
- Gong GC, Liu KK, Chiang KP, Hsiung TM, Chang J, Chen CC, Hung CC, Chou WC, Chung CC, Chen HY, Shiah FK, Tsai AY, Hsieh CH, Shiao JC, Tseng CM, Hsu SC, Lee HJ, Lee MA, Lin II, Tsai FJ. 2011. Yangtze River floods enhance coastal ocean phytoplankton biomass and potential fish production. *Geophys Res Lett* 38:L13603.
- Gong GC, Wen YH, Wang BW, Liu GJ. 2003. Seasonal variation of chlorophyll *a* concentration, primary production and environmental conditions in the subtropical East China Sea. *Deep Sea Res Part II* 50:1219–36.
- Guo C, Liu HB, Zheng LP, Song SQ, Chen BZ, Huang BQ. 2014a. Seasonal and spatial patterns of picophytoplankton growth, grazing and distribution in the East China Sea. *Biogeosciences* 11:1847–62.
- Guo SJ, Feng YY, Wang L, Dai MH, Liu ZL, Bai Y, Sun J. 2014b. Seasonal variation in the phytoplankton community of a continental-shelf sea: the East China Sea. *Mar Ecol Prog Ser* 516:103–26.
- Han AQ, Dai MH, Kao SJ, Gan JP, Li Q, Wang LF, Zhai WD, Wang L. 2012. Nutrient dynamics and biological consumption in a large continental shelf system under the influence of both a river plume and coastal upwelling. *Limnol Oceanogr* 57:486–502.
- Hastie T, Tibshirani R. 1986. Generalized additive models. *Stat Sci* 1:297–310.
- Higgins HW, Wright SW, Schlüter L. 2011. Quantitative interpretation of chemotaxonomic pigment data. In: Roy S, Llewellyn CA, Egeland ES, Johnsen G, Eds. *Phytoplankton pigments*. Cambridge: Cambridge University Press.
- Irwin AJ, Nelles AM, Finkel ZV. 2012. Phytoplankton niches estimated from field data. *Limnol Oceanogr* 57:787–97.
- Jiang Z, Liu J, Chen J, Chen Q, Yan X, Xuan J, Zeng J. 2014. Responses of summer phytoplankton community to drastic environmental changes in the Changjiang (Yangtze River) estuary during the past 50 years. *Water Res* 54:1–11.
- Jiao N, Yang Y, Hong N, Ma Y, Harada S, Koshikawa H, Watanabe M. 2005. Dynamics of autotrophic picoplankton and heterotrophic bacteria in the East China Sea. *Cont Shelf Res* 25:1265–79.
- Jiao NZ, Yang YH, Koshikawa H, Watanabe M. 2002. Influence of hydrographic conditions on picoplankton distribution in the East China Sea. *Aquat Microb Ecol* 30:37–48.
- Jiao NZ, Yang YH, Mann E, Chisholm SW, Chen NH. 1998. Winter presence of *Prochlorococcus* in the East China Sea. *Chin Sci Bull* 43:877–8.
- Kim IN, Lee K, Gruber N, Karl DM, Bullister JL, Yang S, Kim TW. 2014. Increasing anthropogenic nitrogen in the North Pacific Ocean. *Science* 346:1102–6.
- Latasa M. 2007. Improving estimations of phytoplankton class abundances using CHEMTAX. *Mar Ecol Prog Ser* 329:13–21.
- Lin YC, Chung CC, Gong GC, Chiang KP. 2014. Diversity and abundance of haptophytes in the East China Sea. *Aquat Microb Ecol* 72:227–40.
- Litchman E, Klausmeier CA, Schofield OM, Falkowski PG. 2007. The role of functional traits and trade-offs in structuring phytoplankton communities: scaling from cellular to ecosystem level. *Ecol Lett* 10:1170–81.
- Liu SM, Hong GH, Zhang J, Ye XW, Jiang XL. 2009. Nutrient budgets for large Chinese estuaries. *Biogeosciences* 6:2245–63.
- Liu X, Chiang KP, Liu SM, Wei H, Zhao Y, Huang BQ. 2015a. Influence of the Yellow Sea warm current on phytoplankton community in the central Yellow Sea. *Deep Sea Res Part I* 106:17–29.
- Liu X, Huang BQ, Huang Q, Wang L, Ni XB, Tang QS, Sun S, Wei H, Liu SM, Li CL, Sun J. 2015b. Seasonal phytoplankton response to physical processes in the southern Yellow Sea. *J Sea Res* 95:45–55.
- Liu X, Huang BQ, Liu ZY, Wang L, Wei H, Li CL, Huang Q. 2012. High-resolution phytoplankton diel variations in the summer stratified central Yellow Sea. *J Oceanogr* 68:913–27.
- Mackey MD, Mackey DJ, Higgins HW, Wright SW. 1996. CHEMTAX: A program for estimating class abundances from chemical markers—Application to HPLC measurements of phytoplankton. *Mar Ecol Prog Ser* 144:265–83.
- McKie-Krisberg ZM, Sanders RW. 2014. Phagotrophy by the picoeukaryotic green alga *Micromonas*: implications for Arctic Oceans. *ISME J* 8:1953–61.
- Mitra A, Flynn KJ, Burkholder JM, Berge T, Calbet A, Raven JA, Granéli E, Glibert PM, Hansen PJ, Stoecker DK, Thingstad F, Tillmann U, Våge S, Wilken S, Zubkov MV. 2014. The role of mixotrophic protists in the biological carbon pump. *Biogeosciences* 11:995–1005.
- Moran XAG, Lopez-Urrutia A, Calvo-Diaz A, Li WKW. 2010. Increasing importance of small phytoplankton in a warmer ocean. *Glob Chang Biol* 16:1137–44.
- Ning X, Liu Z, Cai Y, Fang M. 1998. Physicobiological oceanographic remote sensing of the East China Sea: Satellite and in situ observations. *J Geophys Res Oceans* 103:21623–35.
- Oksanen J. 2015. Vegan: an introduction to ordination. <http://cran.r-project.org/web/packages/vegan/vignettes/intro-vegan.pdf>.
- Partensky F, Blanchot J, Vaulot D. 1999. Differential distribution and ecology of *Prochlorococcus* and *Synechococcus* in oceanic waters : a review. *Bulletin de l'Institut océanographique, Monaco. Numero Spec* 19:457–75.
- Sommer U. 1984. The paradox of the plankton: fluctuations of phosphorus availability maintain diversity of phytoplankton in flow-through cultures. *Limnol Oceanogr* 29:633–6.
- Tang DL, Di BP, Wei GF, Ni IH, Oh IS, Wang SF. 2006. Spatial, seasonal and species variations of harmful algal blooms in the South Yellow Sea and East China Sea. *Hydrobiologia* 568:245–53.
- R Development Core Team. 2015. R: a language and environment for statistical computing. Vienna: R Foundation for Statistical Computing. Open access available at: <http://cran.r-project.org>.
- Ter Braak CJ. 1986. Canonical correspondence analysis: a new eigenvector technique for multivariate direct gradient analysis. *Ecology* 67:1167–79.
- Thomson RE, Fine IV. 2003. Estimating mixed layer depth from oceanic profile data. *J Atmos Ocean Technol* 20:319–29.
- Wood S. 2006. *Generalized additive models: an introduction with R*. Boca Raton: CRC Press.
- Xie YY, Tilstone GH, Widdicombe C, Woodward EMS, Harris C, Barnes MK. 2015. Effect of increases in temperature and nutrients on phytoplankton community structure and photosynthesis in the western English Channel. *Mar Ecol Prog Ser* 519:61–73.

- Yamaguchi H, Ishizaka J, Siswanto E, Son YB, Yoo S, Kiyomoto Y. 2013. Seasonal and spring interannual variations in satellite-observed chlorophyll-*a* in the Yellow and East China Seas: new datasets with reduced interference from high concentration of resuspended sediment. *Cont Shelf Res* 59:1–9.
- Yamaguchi H, Kim H-C, Son YB, Kim SW, Okamura K, Kiyomoto Y, Ishizaka J. 2012. Seasonal and summer interannual variations of SeaWiFS chlorophyll *a* in the Yellow Sea and East China Sea. *Prog Oceanogr* 105:22–9.
- Zapata M, Rodriguez F, Garrido JL. 2000. Separation of chlorophylls and carotenoids from marine phytoplankton: a new HPLC method using a reversed phase C<sub>8</sub> column and pyridine-containing mobile phases. *Mar Ecol Prog Ser* 195:29–45.
- Zhang C, Hu C, Shang S, Mullerkarger F, Li Y, Dai M, Huang B, Ning X, Hong H. 2006. Bridging between SeaWiFS and MODIS for continuity of chlorophyll-*a* concentration assessments off Southeastern China. *Remote Sens Environ* 102:250–63.
- Zheng L, Chen B, Liu X, Huang B, Liu H, Song S. 2015. Seasonal variations in the effect of microzooplankton grazing on phytoplankton in the East China Sea. *Cont Shelf Res*. doi:10.1016/j.csr.2015.08.010.
- Zhou MJ, Shen ZL, Yu RC. 2008. Responses of a coastal phytoplankton community to increased nutrient input from the Changjiang (Yangtze) river. *Cont Shelf Res* 28:1483–9.
- Zubkov MV, Tarran GA. 2008. High bacterivory by the smallest phytoplankton in the North Atlantic Ocean. *Nature* 455:224–6.
- Zuur AF, Ieno EN, Smith GM. 2007. *Analysing ecological data*. New York: Springer.
- Zwirgmaier K, Jardillier L, Ostrowski M, Mazard S, Garczarek L, Vaulot D, Not F, Massana R, Ulloa O, Scanlan DJ. 2008. Global phylogeography of marine *Synechococcus* and *Prochlorococcus* reveals a distinct partitioning of lineages among oceanic biomes. *Environ Microbiol* 10:147–61.